Atmos. Chem. Phys. Discuss., 11, 14233–14258, 2011
www.atmos-chem-phys-discuss.net/11/14233/2011/
doi:10.5194/acpd-11-14233-2011

Atmospheric
Chemistry
and Physics
Discussions

Multiple-sulfur isotope effects during photolysis of carbonyl sulfide

Y. Lin[1,*], M. S. Sim[1], and S. Ono[1]

[1] Department of Earth, Atmospheric and Planetary Sciences, Massachusetts Institute of Technology, 77 Massachusetts Avenue, Cambridge, MA 02139, USA
[*] now at: School of Earth Sciences and Engineering, Nanjing University, Nanjing, Jiangsu 210093, China

Received: 23 April 2011 – Accepted: 27 April 2011 – Published: 9 May 2011

Correspondence to: Y. Lin (yinglin@nju.edu.cn)

Published by Copernicus Publications on behalf of the European Geosciences Union.

Abstract

Laboratory experiments were carried out to determine sulfur isotope effects during ultraviolet photolysis of carbonyl sulfide (OCS) to carbon monoxide (CO) and elemental sulfur (S^0). The OCS gas at 3.7 to 501 mbar was irradiated with or without a N_2 bath gas using a 150 W Xe arc lamp. Sulfur isotope ratios for the product S^0 and residual OCS were analyzed by an isotope ratio mass-spectrometer with SF_6 as the analyte gas. The isotope effect after correction for the reservoir effects is −6.8 ‰ for the ratio $^{34}S/^{32}S$, where product S^0 is depleted in heavy isotopes. The magnitude of the overall isotope effect is not sensitive to the addition of N_2 but increases to −9.5 ‰ when radiation of $\lambda > 285$ nm is used. The measured isotope effect reflects that of photolysis as well as the subsequent sulfur abstraction (from OCS) reaction. The magnitude of isotope effects for the abstraction reaction is estimated by transition state theory to be between −18.9 and −3.1 ‰ for ^{34}S which gives the photolysis isotope effect as −10.5 to +5.3 ‰. The measured isotope effects are found to be $\delta^{33}S/\delta^{34}S = 0.534 \pm 0.005$ and $\delta^{36}S/\delta^{34}S = 1.980 \pm 0.021$. These values are largely mass-dependent but statistically differ from canonical values for mass-dependent fractionation of 0.515 and 1.90, respectively. The result demonstrates that the OCS photolysis may not produce large isotope effect of more than about 10 ‰, and can be the major source of background stratospheric sulfate aerosol (SSA) during volcanic quiescence.

1 Introduction

Carbonyl sulfide (OCS) accounts for more than 80 % of gas-phase sulfur above 8 km as the most resistant sulfur species to oxidation in the troposphere (e.g. Farwell, 1995; Turco et al., 1980; Khalil and Rasmussen, 1984; Crutzen, 1976). The low solubility and long atmospheric lifetime (about 4 years) with respect to tropospheric chemistry and photolysis enables a significant fraction of OCS to reach the stratosphere (Blake et al., 2008; Pandis et al., 1995; Chin and Davis, 1995; Barkley et al., 2008). OCS exhibits a continuum ultraviolet (UV) absorption spectrum from 200 to 260 nm. Upon UV irradiation in this wavelength range, OCS photodissociates to carbon monoxide and elemental sulfur (S^0) with total quantum yield (Φ) close to 1:

$$\mathrm{OCS} + h\nu \rightarrow \mathrm{S} + \mathrm{CO} \tag{R1}$$

The sulfur atom is oxidized by $OH/O_3/O_2$ to SO_2 and forms sulfate, and is thought to contribute to the stratospheric sulfate aerosol layer (Junge layer) (Junge et al., 1961; Crutzen, 1976; Pitari et al., 2002). The stratospheric sulfate aerosol (SSA) layer at 17–30 km, with lifetime of 3–4 years, affects the atmospheric radiation balance and catalyzes heterogeneous reactions that recycle the inert halogen species related to the ozone budget (e.g. Junge et al., 1961; Danielache et al., 2008; Crutzen, 1976; Turco et al., 1980; Griffith et al., 2000; Rahn and Wahlen, 1997). Understanding the sources and sinks for SSA is of societal importance because artificial formation of SSA is suggested as one potential approach to manage solar radiation in order to mitigate the global warming by carbon dioxide (e.g., Robock et al., 2008). The other significant sources of SSA are oxidation of volcanic SO_2 transported upward from the lower troposphere in deep-convective events (Weisenstein et al., 1997), uplifted tropospheric H_2SO_4 (Pitari et al., 2002), and stratospheric injection of SO_2 by explosive volcanism (Castleman et al., 1973; Pyle et al., 1996). During volcanic quiescence, SO_2 and OCS were assessed to contribute about equally to the stratospheric sulfur budget, but significant uncertainty remains (e.g., SPARC, 2006).

The studies of sulfur isotope ($^{32}S/^{33}S/^{34}S/^{36}S$) ratios may provide important constraints on the sources of SSA if source isotope signatures and isotope effects during chemical conversions are characterized. Leung et al. (2002) and Colussi et al. (2004) suggested relatively large isotope effects of (73.8±8.6) ‰ and (67±7) ‰, respectively, for δ^{34} the UV photolysis of OCS. These values suggest SSA would be highly enriched in ^{34}S if OCS photolysis were the main source for the SSA. Since the background SSA yields only small enrichments of (2.6±0.3) ‰ ($\delta^{34}S_{CDT}$) (Castleman et al., 1973), it was concluded that the contribution of OCS to SSA is either negligible or must be balanced by severely ^{34}S-depleted species, such as sulfate produced from SO_2 (Leung et al., 2002; Colussi et al., 2004). Recent calculation employing wavepacket dynamics, however, showed that sulfur isotope substitution has little effect on the UV cross sections of OCS, and discounted the large isotope effect suggested by Colussi et al. (2004) (Danielache et al., 2009). Therefore, one objective of this study is to measure the isotope fractionation during OCS photolysis reaction by simple laboratory experiments.

Our study also focuses on the rare and non-conventional isotopes of sulfur (^{33}S and ^{36}S) because certain gas phase reactions, SO_2 photolysis and CS_2 photopolymerization, are known to produce mass-independent isotope effects (Farquhar et al., 2001; Colman et al., 1996; Zmolek et al., 1999). Mass-independent isotope effect refers to an isotope effect that does not follow conventional mass-scaling law. That is, the isotope fractionation for the ratio $^{33}S/^{32}S$ is about a half of $^{34}S/^{32}S$ and $^{36}S/^{32}S$ is about twice as much as that of $^{34}S/^{32}S$. More precisely, $\ln(^{33}\alpha) = {}^{33}\theta \ln(^{34}\alpha)$ and $\ln(^{36}\alpha) = {}^{36}\theta \ln(^{34}\alpha)$, where $^{x}\alpha$ is the isotope fractionation factor for the ratio $^{x}S/^{32}S$, where $^{33}\theta$ and $^{36}\theta$ are 0.515 and 1.90, respectively (Hulston and Thode, 1965). The signatures of S-MIF (mass-independent fractionation) have been found exclusively in Archean rocks (e.g. Farquhar et al., 2000; Ono et al., 2003) and SSA deposited in polar ice after major volcanic events (Savarino et al., 2003; Baroni et al., 2007). Although photolysis of SO_2 is thought to be the source reaction for these S-MIF signatures, the physical origin of this unconventional sulfur isotope effect is poorly understood (Farquhar et al., 2001). Given that OCS could have been an important atmospheric sulfur gas in the Archean (Ueno et al., 2009) as well as an important contributor for SSA, it is important to test whether the isotope effect during the photolysis of OCS follows a mass-dependent law.

Therefore, this study has three objectives. The first is to fill the gap in isotope fractionation factor during OCS photolysis by carrying out laboratory photochemical experiments, the second is to test if OCS photolysis follows the conventional mass-dependent law by determining multiple-sulfur isotope fractionation factors, and the third is to test whether OCS contributes to SSA.

2 Experimental set up

A 150 watt Xenon arc lamp (Newport Model 6254) with lamp housing (Newport Model 67005) was used as a light source. The Xenon arc lamp has irradiance of about 1.5 mW m^{-2} nm^{-1} at 200 nm, increasing to 10.5 mW m^{-2} nm^{-1} at 300 nm. The photochemical reaction cell is a 30-cm-long, 48-mm-ID glass cylinder equipped with optical grade quartz windows (Aceglass Model 7894-35). The transmittance of the window is 40 % at 200 nm, increasing to 90 % at 300 nm. For wavelength λ>285 nm experiments, an Oriel colored glass filter (Newport Model 59423) was used. Commercial carbonyl sulfide (≥97.5 % pure, Sigma Aldrich) was used for this study as the reactant. The gas chromatography (1/8-inch-OD column packed with SupelcoChromosil 310) analysis by a TCD detector showed that most impurity is composed of CO_2 (2.5 %).

The OCS was introduced to the photochemical cell through a glass vacuum line. Pressures for the initial OCS, residual OCS, and product CO were monitored by a capacitance manometer. In all experiments, yellowish elemental sulfur (S^0) condensed on the inner surfaces of the windows and the photochemical cell. After photolysis, residual OCS was collected at liquid nitrogen temperature. The OCS (initial or residual) was hydrolyzed in alkaline zinc solution (0.14 mol/l zinc acetate in 2 mol/l NaOH), and precipitated as ZnS. The ZnS was precipitated as Ag_2S by 0.1 mol/l $AgNO_3$ after neutralizing with zinc acetate solution. The S^0 precipitated inside the photochemical cell was dissolved in about 50 ml dichloromethane (DCM). After evaporating DCM, S^0 was reduced by chromium chloride following Canfield et al. (1986), and was precipitated as Ag_2S.

The isotope ratio analysis was carried out in the stable isotope laboratory at MIT with a procedure similar to the one described in Ono et al. (2006). Approximately 2 mg of silver sulfide was reacted with elemental fluorine (about 70 mbar) for over 6 h at 300 ∘C. The product SF_6 was purified by a preparative gas chromatography equipped with a packed column of Molesieve 5A and Hayesep Q. Isotope ratios were analyzed by an isotope ratio mass spectrometer (Thermo-electron MAT 253) by measuring ions

$^{32}SF_5^+$, $^{33}SF_5^+$, $^{34}SF_5^+$, and $^{36}SF_5^+$. Six replicated analyses of OCS yield 2σ standard deviations of 0.26, 0.53, and 1.05 ‰ for $\delta^{33}S$, $\delta^{34}S$, and $\delta^{36}S$, respectively. These numbers represent errors for gas handling, wet chemistry (hydration and precipitation), fluorination, and mass spectrometer analysis. Errors in $\delta^{33}S$, $\delta^{34}S$, and $\delta^{36}S$ are mass-dependently correlated.

3 Results

Sulfur isotope ratios are reported by conventional delta notation:

$$\delta^{x}S = \left(\frac{^{x}R_{\text{sample}}}{^{x}R_{\text{reference}}} - 1\right) \times 1000 \tag{1}$$

where $^{x}R_{\text{sample}}$ is the isotope ratio ($^{x}S/^{32}S$, where x = 33, 34, or 36) of product S^0 or residual OCS and $^{x}R_{\text{reference}}$ is that of initial OCS.

Results for 12 UV photolysis of OCS are shown in Table 1. Residual OCS is enriched in ^{34}S up to 4.43 ‰ except for 11–28, which is taken as an experimental error due to low S^0 yield for the long-duration run. The photolysis product S^0 is depleted in $\delta^{34}S$ by 2.24 to 6.72 ‰ with respect to initial OCS. Because isotope ratios of reactant OCS change during photolysis, the isotope fractionation factor for the photodissociation is calculated using an approximated formula of Rayleigh distillation (Mariotti et al., 1981):

$$^{34}\varepsilon = \frac{f-1}{f\ln(f)}\delta^{34}S_S \tag{2}$$

where, $^{34}\varepsilon$, $\delta^{34}S_S$, and f are isotope enrichment factor, isotopic composition of S^0 at the end of the run, and the fraction of residual OCS, respectively. In this definition, a negative value of ε indicates that the product S^0 is depleted in ^{34}S. The value for f is derived from S^0 yield and initial OCS gas pressure, or from isotope mass balance for runs where isotope compositions for both residual OCS and S^0 are measured. The two $^{34}\varepsilon$ estimates are largely consistent, in particular, in runs 10-02, 10-03, and 11-11 (Table 1). The two f values differ for the run 11-05, likely due to error in pressure measurements.

For pure OCS experiments, isotope effects ($^{34}\varepsilon$) of (−6.8±0.2) ‰ are derived for the best set of experiments (10-02 and 11-11). These two results represent the low S^0 yield (i.e., small reservoir size correction), and consistent f values. Addition of N_2 (experiments 10-19, 11-10, and 11-12) yields $^{34}\varepsilon$ of −6.8 to −5.3 ‰, showing that addition of N_2 has little or no effect on the isotope fractionation factor. The experiment 11-28 with $\lambda > 285$ nm radiation yields a slightly larger isotope effect of −9.5 ‰.

When all data are plotted in $\ln(\delta^{33}S+1)$ vs. $\ln(\delta^{34}S+1)$ and $\ln(\delta^{36}S+1)$ vs. $\ln(\delta^{34}S+1)$ diagrams, the least square fit slopes are 0.534±0.005 and 1.980± 0.021, respectively (Fig. 1). The log scale is used here to take into account the power law relationship of mass-dependent fractionation (e.g., Luz and Barkan, 2005). The standard errors are derived from linear regression and depend on residuals of the fits and degree-of-freedom (*df*) of the residuals, both derived by ANOVA (Analysis of Variance) in statistical program SPSS. These mass-dependent exponents are largely mass-dependent but statistically different from the canonical mass-dependent values of 0.515 and 1.90, respectively, for $\delta^{33}S/\delta^{34}S$ and $\delta^{36}S/\delta^{34}S$ (Hulston and Thode, 1965; Otake et al., 2008).

4 Discussion

4.1 Sulfur isotope effects for laboratory OCS photolysis experiments

For laboratory OCS photochemistry experiments employed in this study, photodissociation of OCS (Reaction R1) is followed by sulfur abstraction from OCS (Reaction R2) (Basco and Pearson, 1967; Breckenridge and Taube, 1970; Wiebe et al., 1964; Zhao et al., 1995):

$$OCS + S \rightarrow S_2 + CO \tag{R2}$$

If the rates of both reactions (R1) and (R2) are sensitive to sulfur isotope substitution, the measured isotope effects would be the average of the isotope effects associated with the two reactions. For ^{34}S, that is:

$$^{34}\varepsilon = 1/2(^{34}\varepsilon_1 + ^{34}\varepsilon_2) \tag{3}$$

where $^{34}\varepsilon_1$ and $^{34}\varepsilon_2$ are isotope enrichment factors due to photolysis (R1) and sulfur abstraction Reaction (R2), respectively. The factor 1/2 reflects two sulfur atoms in S_2. Assuming intermediate steady state condition for atomic S, the mass of atomic sulfur in the Reaction (R2) (i.e., OCS + ^{32}S versus OCS + ^{34}S) does not produce isotope effects in the overall product. Thus, $^{34}\varepsilon_2$ represents the difference in the reaction rates between $OC^{34}S$ + S and $OC^{32}S$ + S. In order to gain constraints on the isotope effect for UV photolysis, we will first estimate the isotope effect during sulfur abstraction reaction.

4.2 Sulfur isotopic effects during sulfur abstraction reaction

The OCS photolysis (Reaction R1) produces S in both singlet and triplet states. The isotope effect associated with the sulfur abstraction reaction ($^{34}\varepsilon_2$) may depend on the spin state of S atom since the reaction follows either a singlet or triplet potential energy surface (Lu et al., 2006). Three sets of experiments were designed to assess the different S_2 formation channels to elucidate the systematics of isotope fractionation.

In experiments with $\lambda > 200$ nm, without N_2 bath gas, the reactions are:

$$OCS + h\nu \rightarrow CO + S(^1D) \tag{R1a}$$

$$OCS + h\nu \rightarrow CO + S(^3P) \tag{R1b}$$

$$S(^1D) + OCS \rightarrow CO + S_2 \tag{R2a}$$

$$S(^3P) + OCS \rightarrow CO + S_2 \tag{R2b}$$

$$S(^1D) + OCS \rightarrow OCS + S(^3P) \tag{R3}$$

During photolysis (R1), atomic sulfur is produced predominantly in $S(^1D)$ electronic state ($\Phi_{1a} = 0.74$) because production of $S(^3P)$ is spin forbidden (Okabe, 1978; Sidhu et al., 1966; Breckenridge and Taube, 1970). Pseudo-first-order rate constants for Reactions (R2a), (R2b), and (R3) were estimated to be 5×10^{-11}, 2.7×10^{-15}, and 15×10^{-11} cm^3 molecule^{-1} s^{-1}, respectively (Zhao et al., 1995; Lu et al., 2006). Given these rate constants, approximately one fifth of S_2 is formed through abstraction reaction with $S(^1D)$ and the rest is from $S(^3P)$ channel.

The addition of inert gas (N_2) in the second set of experiments would quench $S(^1D)$:

$$S(^1D) + N_2 \rightarrow N_2 + S(^3P) \tag{R4}$$

Rate constant for the Reaction (R4) is estimated to be 8×10^{-11} cm^3 molecule^{-1} s^{-1} (Zhao et al., 1995). Under the experimental conditions (53.3 to 400 mbar N_2), the production of S_2 is exclusively from $S(^3P)$ channel (Reaction R2b). The S_2 recombination reaction:

$$2S(^3P) + N_2 \rightarrow N_2 + S_2 \tag{R5}$$

is slow (second-order rate constant is about 10^{-33} cm^6 molecules^{-2} s^{-1} (Du et al., 2008) and is only relevant if a high power UV source is used (Breckenridge and Taube, 1970). Because dissociation threshold through $S(^1D)$ channel (Reaction R1a) is (4.26±0.1) eV or (291±7) nm (Suzuki et al., 1998), photolysis of OCS with $\lambda>285$ nm produces S^0 exclusively in the triplet state (Reaction R1b).

The experimental results show that addition of N_2 does not significantly affect the overall isotope effect during OCS photolysis; $^{34}\varepsilon$ is −6.8‰ for pure OCS photolysis versus −6.8 to −5.3 ‰ for OCS photolysis with addition of N_2 (Table 1). These similar ranges of isotope enrichments suggest that spin states have little effect on the isotope fractionation for the abstraction reaction. It will be discussed in the next section that the relatively larger magnitude isotope effect of −9.5 ‰ for the photolysis with $\lambda > 285$ nm, is likely due to photolysis itself rather than due to spin chemistry.

The isotope effect for sulfur abstraction reaction ($^{34}\varepsilon_2$) is estimated by applying transition state theory (Van Hook, 1970; Tanaka et al., 1996). Lu et al. (2006) showed a number of possible transition states for the atomic S abstraction reactions (R2a&b). We used two of their transition states (TS1 and TS2) as representative transition state structures. The transition structure TS1 represents the main channel for the abstraction reaction, where atomic S is attached to S in OCS forming a bent OC-S-S molecule. The transition state, TS2, is a minor channel but two S are attached to carbon forming a triangular O-C-S_2 molecule (Lu et al., 2006). Vibrational frequencies for the ground state OCS and two transition states are calculated for four sulfur isotopologues at B3LYP/6-311+G(3df) level with Gaussian03. The estimated frequencies for OCS are scaled by 0.9793, 0.9705, and 0.9638 for bending, CS stretching, and OC stretching vibrational modes, respectively, to match experimental frequencies by Masukidi et al. (1992). Frequencies for TS1 and TS2 are estimated by using the geometry reported by Lu et al. (2006). The calculated vibrational frequencies with reported geometry reproduce reported vibrational frequencies at ±0.3 % for TS2 but are different by 7% for TS1. The $^{34}\varepsilon_2$ are estimated to be −18.9 ‰ and −3.1 ‰ for abstraction reaction via TS1 and TS2, respectively (Table 2). The calculated isotope effects are mass-dependent with $^{33}\theta$ and $^{36}\theta$ values of 0.5138±0.0006 and 1.905±0.005, respectively (Table 2).

Photochemical experiments using doubly isotope substituted carbonyl sulfide ($^{18}OC^{34}S$) show small degree of isotope exchange through atomic sulfur (Breckenridge and Taube, 1970):

$$OC^{32}S + {}^{34}S \rightleftharpoons OC^{34}S + {}^{32}S \tag{R6}$$

Using the conventional formula (Bigeleisen and Mayer, 1947) and the estimated vibrational frequencies for OCS, the equilibrium constant for the reaction (R6) is estimated to be 1.0175. Thus, isotope exchange Reaction (R6), when completed, S would be −17.2 ‰ depleted with respect to OCS in ^{34}S. The extent of isotope exchange, however, is minor and is approximately 6 % with respect to the photolysis yield (Breckenridge and Taube, 1970). Following the formula by Ohmoto and Lasaga (1982), the isotope exchange of about 6 % may contribute at most 0.7 ‰ additional decrease in $^{34}\varepsilon_2$; exact magnitude depends upon the initial isotopic compositions. Because the effect is small, the isotope exchange Reaction (R6) is not taken into account for the further analysis because the magnitude of the effect is small compared to that of photolysis and abstraction reactions.

With average $^{34}\varepsilon$ values of −6.8 ‰, using Eq. (3), isotope effects due to photolysis ($^{34}\varepsilon_1$) are estimated to be +5.3 ‰ if transition structure TS1 is assumed (i.e., $^{34}\varepsilon_2 = -18.9$ ‰) and −10.5 ‰ if transition structure TS2 is assumed (i.e., $^{34}\varepsilon_2 = -3.1$ ‰). Although the results do not constrain the sign of the $^{34}\varepsilon_1$, our experimental data demonstrate that OCS photolysis is not likely a source of large (about +67 ‰) isotope effect as previously suggested by Colussi et al. (2004).

4.3 Sulfur isotope effects during photolysis of OCS

Sulfur isotope effects for photolysis can be estimated from ZPE-shift method of Miller and Yung (2000) for the condition applied for the experiments (Colussi et al., 2004; Danielache et al., 2009). For a given experimental pressure, the isotopologue specific photodissociation rate constant is a function of the path length (z) and wavelength (λ):

$$^{x}J(\lambda,z) = {}^{x}\Phi(\lambda)\,{}^{x}\sigma(\lambda)F_0 e^{-\sigma_{\mathrm{OCS}}mz} \tag{4}$$

where, x represents each isotope (i.e., x = 32, 33, 34, or 36), Φ is the photolysis quantum yield (assumed to be unity), σ is the absorption cross section, and F_0, is a photon flux at the photocell window (i.e., at optical depth $z = 0$). The last term is to correct opacity by the OCS between the light source and the given optical depth (z), σ_{OCS} and m are the cross section of OCS and concentration of total OCS (all isotopologues), respectively.

Absorption cross sections for minor isotopologues, $\mathrm{OC}^{33}\mathrm{S}$, $\mathrm{OC}^{34}\mathrm{S}$, and $\mathrm{OC}^{36}\mathrm{S}$ can be estimated by blue-shifting $\mathrm{OC}^{32}\mathrm{S}$ cross section following ZPE-shift method of Miller and Yung (2000):

$$^{x}\sigma(E+\Delta\mathrm{ZPE}) = {}^{32}\sigma(E) \tag{5}$$

where E is the photon energy and ΔZPE is the zero point energy difference between major $\mathrm{OC}^{32}\mathrm{S}$ and a given isotopologue. ΔZPE calculated are 3.524, 6.852, and 13.026 cm^{-1} for $\mathrm{OC}^{33}\mathrm{S}$, $\mathrm{OC}^{34}\mathrm{S}$, and $\mathrm{OC}^{36}\mathrm{S}$, respectively.

The OCS absorption spectrum of Molina et al. (1981) is shown in Fig. 2b. That is taken as $^{32}\mathrm{OCS}$ and is approximated by a function of the form:

$$^{32}\sigma = \exp\left(\sum_{n=0}^{6} A_n \lambda^n\right) \tag{6}$$

where various A are constants. Equations (5) and (6) are used to estimate the ratios of isotopologue specific cross sections (e.g., $^{33}\sigma/^{32}\sigma$, $^{34}\sigma/^{32}\sigma$, and $^{36}\sigma/^{32}\sigma$). Equation (4) is integrated to the wavelength range, from 190 to 280 nm, and to the photochemical cell length (i.e., $z = 0$ to 30 cm) to estimate ε_1 for the experimental conditions by Eq. (7) (Miller et al., 2005). Results are shown in Table 3.

$$\varepsilon_1 = \left(\frac{J'}{J} - 1\right) \tag{7}$$

where J and J are the photodissociation rate constant of $^{32}\mathrm{S}$ and those of substituted isotopologues $^{33}\mathrm{S}$, $^{34}\mathrm{S}$, and $^{36}\mathrm{S}$, respectively.

The magnitude (and sign) of the expected isotope effects depends upon the irradiance spectrum determined by the light source and window material. The wavelength dependence for the isotope effects are intensively studied for nitrous oxide photolysis

Title Page
Abstract | Introduction
Conclusions | References
Tables | Figures
◀| |▶
◀ ▶
Back | Close
Full Screen / Esc
Printer-friendly Version
Interactive Discussion

(Kaiser et al., 2003). This is because the ZPE-shift method suggests the sign of the isotope effect changes at the maximum absorption at 222 nm (Fig. 2c). The estimated fractionation factor is positive (product ^{34}S-enriched) for photolysis with $\lambda<222$ nm and negative (product ^{34}S-depleted) for photolysis with $\lambda>222$ nm. The photon flux (F_0) for the Xe arc lamp was given by the manufacture's datasheet and was corrected for measured transmittance for the window material. Calculated total photolysis rate constant (i.e., $^{32}J+^{33}J+^{34}J+^{36}J$) is shown in Fig. 2d at varying total pressures of OCS. The rate constant shows maximum at 226 nm at total pressure of OCS of 2.7 mbar. This is slightly higher than the maximum OCS cross section at 222 nm because of the increasing photon flux from the Xe arc lamp with increasing wavelength (Fig. 2a). The $^{34}\varepsilon_1$ values calculated by ZPE-shift method are −2.2 ‰ at OCS gas pressure of 26.7 mbar and −4.1 ‰ at OCS gas pressure of 400 mbar, both at wavelength region of 190–280 nm (Table 3). The isotope effect is a weak function of the pressure because a part of UV absorption saturates at higher OCS pressures such that maximum absorption shifts to longer wavelength (Fig. 2d). The ratios of ε_1 values give mass-dependent exponents of 0.514 and 1.90 for $^{33}\theta$ and $^{36}\theta$, respectively. The mass-dependence for the ZPE-shift method is expected since estimated ZPE shift is inherently mass-dependent.

The ZPE-shift method predicts a large negative isotope effect of −10.1 ‰ for $^{34}\varepsilon_1$ with irradiance at 280 nm (Fig. 2c). This is consistent with the relatively large magnitude fractionation measured for photolysis with $\lambda>285$ nm compared to full spectrum experiments. Using the ZPE-shift method to estimate isotope effect with $\lambda>280$ nm is not plausible because the estimation requires accurate determination of absorption spectrum at $\lambda>280$ nm.

Danielache et al. (2009) reported isotopologue specific cross sections estimated from wavepacket dynamics calculation. Predicted isotope effect ($^{34}\varepsilon_1$) is consistent with that of the ZPE-shift method at low energy side (λ longer than about 220 nm) but differs significantly at high energy side of the spectrum (λ shorter than about 220 nm). Danielache et al. (2009) estimated $^{34}\varepsilon_1$ of +4.9 ‰ for the OCS photolysis at 190–250 nm. The predicted isotope effect ($^{34}\varepsilon_1$) is +4.2 ‰ for the light source used in this experiments. If one applies +4.2 ‰ for photolysis isotope effect ($^{34}\varepsilon_1$) and −6.8 ‰ for ($^{34}\varepsilon$), isotope effect associated with sulfur abstraction reaction ($^{34}\varepsilon_2$) is estimated to be −17.8 ‰. This magnitude of the isotope effect agrees well with what is estimated (−18.9 ‰) for one of the transition states (TS1).

4.4 Multiple sulfur isotope effect

Bhattacharya et al. (2000) reported a large magnitude mass-independent isotope fractionation among triple oxygen isotope system (^{16}O-^{17}O-^{18}O) during photolysis of carbon dioxide at 185 nm. They attributed near resonant vibronic coupling between singlet and triplet states to be the source of MIF during the photolysis. The anomalous isotope effect was only observed for spin forbidden dissociation process; the isotope effect follows conventional mass-dependence for the photolysis with λ<160 nm, where CO_2 photodissociates without spin violation. One may expect similar mass-independent isotope effect in sulfur isotope system for the spin-forbidden photolysis process for OCS (Lyons, 2009).

The photolysis of OCS produces predominantly S(^{1}D) without spin violation. Because dissociation threshold through S(^{1}D) channel is about 285 nm, the experiments with λ>285 nm produces S(^{3}P) exclusively through a spin-forbidden process much like the CO_2 photolysis with λ>167 nm. The OCS photolysis with λ>285 nm, however, is largely mass-dependent, suggesting that OCS photolysis through S(^{3}P) channel is mass-dependent. A slight increase in ^{34}S-depletion (−9.5 ‰) for photolysis with λ>285 nm compared to the full spectrum is measured. This is consistent with a simple ZPE-shift method (Miller and Yung, 2000), which is inherently mass-dependent.

The measured mass-dependent exponents of 0.534 and 1.980 for $^{33}\theta$ and $^{36}\theta$, respectively, are statistically different from what are expected for canonical mass dependence of 0.515 and 1.90, suggesting potential mass-independent isotope effects during the OCS photolysis. This potential MIF may be related to shorter wavelength (λ<220 nm) rather than longer wavelength (λ>285 nm) photolysis. Danielache et al. (2009) suggested significant sulfur isotope effects at high energy side of the spectrum (λ<220 nm). They also suggested that forbidden transition from the lowest excited state ($^1\Delta$) and ground state ($^1\Sigma^+$) may be allowed in the bend geometry of excited $2^1A'$–$1^1A'$ states via vibronic coupling. Such vibronic coupling may lead to mass-independent isotope effects during OCS photolysis process.

4.5 Implications to stratospheric sulfur aerosol (SSA)

Castleman et al. (1974) suggested the δ^{34}S of background SSA to be +2.6 ‰. The δ^{34}S value of the tropospheric OCS has not been measured but was estimated to be +11 ‰ (Newman et al., 1991). The photolysis isotope effect of −8.4 ‰ would be expected if the OCS photolysis is the main source of sulfur in SSA. Based upon large $^{34}\varepsilon$ for photolysis of OCS of larger than 67 ‰, Leung et al. (2002) and Colussi et al. (2004) concluded that OCS does not contribute significantly to the SSA or the large positive isotope effect is cancelled out by other sulfur source with highly negative δ^{34}S. Our experimental results demonstrate the OCS photolysis ($^{34}\varepsilon_1$) is unlikely to produce large (>10 ‰) isotope effects, and thus, OCS can be a major contributor for SSA in volcanic quiescent periods.

Ueno et al. (2009) suggested OCS was important greenhouse gas in the early Earth, compensating the Earth's radiation budget under low solar luminosity. If this were the case, OCS is expected to contribute significant S production during the Archean era because OCS absorbs photons to shield SO_2 but it dissociates at quantum efficiency close to unity. This study confirms that the isotope effect during the OCS photolysis and following S abstraction reactions are largely mass-dependent.

In order to further constrain the isotope effect for the OCS photolysis in the stratosphere, future laboratory experiments should focus on the photolysis with λ of about 200 nm because this is the window of UV that becomes available at above 20 km altitude (Minschwaner et al., 1993; DeMore et al., 1997) and where most OCS photolysis is occurring (Colussi et al., 2004). The photolysis experiments with λ of about 200 nm may also provide experimental confirmation for the results of Danielache et al. (2009)

about the deviation of isotope effect from the ZPE-shift method, and potential mass-independent isotope effects in the sulfur isotope system. Our experimental results, however, have direct inference on the long wavelength (λ>270 nm) OCS photolysis that would be potentially important as the fate of tropospheric OCS (Turco et al., 1981).

5 Conclusions

Laboratory photolysis of carbonyl sulfide produced elemental sulfur depleted in heavy isotopes by −6.8 ‰ for the ratio $^{34}S/^{32}S$ relative to initial OCS. Because OCS photolysis reaction is followed by sulfur abstraction reaction (OCS + S → CO + S_2), the measured isotope effect is an average of the effects produced by photolysis and abstraction reactions. The isotope effect for abstraction reaction is estimated by using transition state theory to be −18.9 ‰ (TS1) and −3.1 ‰ (TS2). Therefore, the isotope effect due to photolysis under experimental conditions is constrained to be −10.5 to +5.3 ‰. A relatively small (<10 ‰) isotope effect is consistent with the ZPE-shift method of Miller and Yung (2000) as well as the result of recent wavepacket dynamic calculation by Danielache et al. (2009). The sulfur isotope constraints on the contribution of OCS to the stratospheric sulfate aerosol layer need to be reevaluated.

Mass-dependent exponents, the ratios for the isotope effects, for the 12 experiments are 0.534±0.005 and 1.980±0.021 for $\delta^{33}S/\delta^{34}S$ and $\delta^{36}S/\delta^{34}S$, respectively. These values are statistically different from the canonical values of 0.515 and 1.90, suggesting potential mass-independent isotope effects during OCS photolysis. Further experiments are underway to test if photolysis with λ of about 200 nm, relevant range for stratospheric OCS photolysis, would produce larger and mass-independent isotope effects.

This study demonstrates that simple laboratory photochemical experiments, theoretical quantum physics, and spectroscopic experiments (i.e., absorption cross section measurements for pure isotopologues) are complimentary to each other, and often required to untangle isotope effects in complex photochemical processes.

Acknowledgements. William J. Olszewski contributed to the construction of sulfur fluorination line, the automated purification line for SF_6 and the associated control program. Sebastian Danielache shared his calculation of ε values based on theoretical spectra. The authors have heartfelt gratitude. This project was partly funded by NASA Exobiology program.

References

Barkley, M. P., Palmer, P. E., Boone, C. D., and Bernath, P. F.: Global distributions of carbonyl sulfide in the upper troposphere and stratosphere, Geophys. Res. Lett., 35, L14810, doi:10.1029/2008GL034270, 2008.

Baroni, M., Thiemens, M. H., Delmas, R. J., and Savarino, J.: Mass-independent sulfur isotopic compositions in stratospheric volcanic eruptions, Science, 315, 84–87, 2007.

Basco, N. and Pearson, A. E.: Reactions of sulphur atoms in presence of carbon disulphide, carbonyl sulphide and nitric oxide, Trans. Faraday Soc., 63, 2684–2694, 1967.

Bhattacharya, S. K., Savarino, J., and Thiemens, M. H.: A new class of oxygen isotopic fractionation in photodissociation of carbon dioxide: Potential implications for atmospheres of Mars and Earth, Geophys. Res. Lett., 27, 1459–1462, 2000.

Bigeleisen, J. and Mayer, M. G.: Calculation of equilibrium constants for isotopic exchange reactions, J. Chem. Phys., 15, 261–267, 1947.

Blake, N. J., Campbell, E., Vay, S. A., Fuelberg, H. E., Huey, L. G., Sachse, G., Meinardi, S., Beyersdorf, A., Baker, A., Barletta, B., Midyett, J., Doezema, L., Kamboures, M., McAdams, J., Novak, B., Rowland, F. S., and Blake, D. R.: Carbonyl sulfide (OCS): Large-scale distributions over North America during INTEX-NA and relationship to CO_2, J. Geophys. Res., 113, D09S90, doi:10.1029/2007JD009163, 2008.

Breckenridge, W. H. and Taube, H.: Some reactions of ground-state (^{3}P) and electronically excited (^{1}D) sulfur atoms, J. Chem. Phys., 53, 1750–1767, 1970.

Canfield, D. E., Raiswell, R., Westrich, J. T., Reaves, C. M., and Berner, R. A.: The use of chromium reduction in the analysis of reduced inorganic sulfur in sediments and shales, Chem. Geol., 54, 149–155, 1986.

Castleman, A. W., Munkelwitz, H. R., and Manowitz, B.: Contribution of volcanic sulphur compounds to the stratospheric aerosol layer, Nature, 244, 345–346, 1973.

Castleman, A. W., Munkelwitz, H. R., and Manowitz, B.: Isotopic studies of the sulfur component of the stratospheric aerosol layer, Tellus, 26, 222–234, 1974.

Chin, M. and Davis, D. D.: A reanalysis of carbonyl sulfide as a source of stratospheric background sulfur aerosol, J. Geophys. Res., 100, 8993–9005, 1995.

Colman, J. J., Xu, X. P., and Thiemens, M. H.: Photopolymerization and mass-independent sulfur isotope fractionations in carbon disulfide, Science, 273, 774–776, 1996.

Colussi, A. J., Leung, F.-Y. T., and Hoffmann, M. R.: Electronic spectra of carbonyl sulfide sulfur isotopologues, Environ. Chem., 1, 44–48, 2004.

Crutzen, P. J.: The possible importance of CSO for the sulfate aerosol layer of the Stratosphere, Geophys. Res. Lett., 3, 73-76, 1976.

Danielache, S. O., Johnson, M. S., Nanbu, S., Grage, M. M.-L., McLinden, C., and Yoshida, N.: Ab initio study of sulfur isotope fractionation in the reaction of OCS with OH, Chem. Phys. Lett., 450, 214–220, 2008.

Danielache, S. O., Nanbu, S., Eskebjerg, C., Johnson, M. S., and Yoshida, N.: Carbonyl sulfide isotopologues: ultraviolet absorption cross sections and stratospheric photolysis, J. Chem. Phys., 131, 024307, doi:10.1063/1.3156314, 2009.

DeMore, W. B., Sanders, S. P., Golden, D. M., Hampson, R. F., Kurylo, M. J., Howard, C. J., Ravishankara, A. R., Kolb, C. E., and Molina, M. J.: Chemical kinetics and photochemical data for use in stratospheric modeling, JPL, evaluation no. 12, California Institute of Technology, Pasadena, California, USA, 1997.

Du, S., Francisco, J. S., Shepler, B. C., and Peterson, K. A.: Determination of the rate constant for sulfur recombination by quasiclassical trajectory calculations, J. Chem. Phys., 128, 204306, doi:10.1063/1.2919569, 2008.

Farquhar, J., Bao, H., and Thiemens, M. H.: Atmospheric influence of the Earth's earliest sulfur cycle, Science, 289, 756–758, 2000.

Farquhar, J., Savarino, J., Airieau, S., and Thiemens, M. H.: Observation of wavelength-sensitive mass-independent sulfur isotope effects during SO_2 photolysis: Applications to the early atmosphere, J. Geophys. Res., 12, 32829–32839, 2001.

Farwell, S. O., MacTaggart, D. L., Chathan, W., Everson, D. O., Samaranayake, K., and Lim, Y. T.: Airborne measurements of total sulfur gases during NASA Global Tropospheric Experiment/Chemical Instrumentation Test and Evaluation 3, J. Geophys. Res., 100, 7223–7234, 1995.

Griffith, D. W. T., Toon, G. C., Sen, B., Blavier, J. F., and Toth, R. A.: Vertical profiles of nitrous oxides isotopomer fractionation measured in the stratosphere, Geophys. Res. Lett., 27, 2485–2488, 2000.

Hulston, J. R. and Thode, H. G.: Variations in the S^{33}, S^{34}, and S^{36} contents of meteorites and their relation to chemical and nuclear effects, J. Geophys. Res., 70, 3475-3484, 1965.

Junge, C. E., Chagnon, C. W., and Manson, J. E.: Stratospheric aerosols, J. Meteorol., 18, 81–108, 1961.

Kaiser, J., Röckmann, T., Brenninkmeijer, C. A. M., and Crutzen, P. J.: Wavelength dependence of isotope fractionation in N_2O photolysis, Atmos. Chem. Phys., 3, 303–313, doi:10.5194/acp-3-303-2003, 2003.

Khalil, M. A. K. and Rasmussen, R. A.: Global sources, lifetimes and mass balances of carbonyl sulfide (OCS) and carbon disulfide (CS_2) in the Earth's atmosphere, Atmos. Environ., 18, 1805–1813, 1984.

Leung, F.-Y. T., Colussi, A. J., Hoffmann, M. R., and Toon, G. C.: Isotopic Fractionation of carbonyl sulfide in the atmosphere: implications for the source of background stratospheric sulfate aerosol, Geophys. Res. Lett., 29, 1474, doi:10.1029/2001GL013955, 2002.

Lu, C.-W., Wu, Y.-J., Lee, Y.-P., Zhu, R. S., and Lin, M. C.: Experimental and theoretical investigation of rate coefficients of the reaction $S(^3P)$ + OCS in the temperature range of 298–985 K, J. Chem. Phys., 125, 164329, 2006.

Luz, B. and Barkan, E.: The isotope ratios $^{17}O/^{16}O$ and $^{18}O/^{16}O$ in molecular oxygen and their significance in biogeochemistry, Geochim. Cosmochim. Acta, 69, 1099–1110, 2005.

Lyons, J. R.: Atmospherically-derived mass-independent sulfur isotope signatures, and incorporation into sediments, Chem. Geol., 267, Sp. Iss. SI, 164–174, 2009.

Mariotti, A., Germon, J. C., Hubert, P., Kaiser, P., Letolle, R., Tardieux, A., and Tardieux, P.: Experimental determination of nitrogen kinetic isotope fractionation: some principles; illustration for the denitrification and nitrification processes, Pl. Soil, 62, 413–430, 1981.

Masukidi, L. S., Lahaye, J. G., and Fayt, A.: Intracavity CO and CO_2 laser Stark spectroscopy of the isotopomers of carbonyl sulfide, J. Mol. Spectrosc., 154, 137–162, 1992.

Miller, C. E., Onorato, R. M., Liang, M.-C., and Yung, Y. L.: Extraordinary isotopic fractionation in ozone photolysis, Geophys. Res. Lett., 32, L14814, doi:10.1029/2005GL023160, 2005.

Miller, C. E. and Yung, Y. L.: Photo-induced isotopic fractionation, J. Geophys. Res., 105, 29039–29051, 2000.

Minschwaner, K., Salawitch, R. J., and McElroy, M. B.: Absorption of solar radiation by O_2: implications for O_3 and lifetimes of N_2O, $CFCl_3$, and CF_2Cl_2, J. Geophys. Res., 98, 10543–

10561, 1993.

Molina, L. T., Lamb, J. J., and Molina, M. J.: Temperature-dependent UV absorption cross-sections for carbonyl sulfide, Geophys. Res. Lett., 8, 1008–1011, 1981.

Newman, L., Krouse, H. R., and Grinenko, V. A.: Sulphur isotope variations in the atmosphere, in Stable Isotopes: Natural and Anthropogenic sulphur in the Environment, edited by: H. R. Krouse and V. A. Grinenko, 133–176, Scientific Committee On Problems of Environment (SCOPE), available online at: http://www.icsu-scope.org/downloadpubs/scope43/index.html, 1991.

Ohmoto, H. and Lasaga A. C.: Kinetics of reactions between aqueous sulfates and sulfides in hydrothermal systems, Geochim. Cosmochim. Acta, 46, 1727–1745, 1982.

Okabe, H.: Photochemistry of small molecules, John Wiley, New York, USA, 215–217, 1978.

Ono, S., Eigenbrode, J. L., Pavlov, A. A., Kharecha, P., Rumble, D., Kasting, J. F., and Freeman, K. H.: New insights into Archean sulfur cycle from mass-independent sulfur isotope records from the Hamersley Basin, Australia, Earth Planet. Sci. Lett., 213, 15–30, 2003.

Ono, S., Wing, B., Johnston, D., Rumble, D., and Farquhar, J.: Mass-dependent fractionation of quadruple stable sulfur isotope system as a new tracer of sulfur biogeochemical cycles, Geochim. Cosmochim. Acta, 70, 2238–2252, 2006.

Otake, T., Lasaga, A. C., and Ohmoto, H.: Ab initio calculations for equilibrium fractionations in multiple sulfur isotope systems, Chem. Geol., 249, 357–376, 2008.

Pandis, S. N., Wexler, A. S., and Seinfeld, J. H.: Dynamics of tropospheric aerosols, J. Phys. Chem., 99, 9646–9659, 1995.

Pitari, G., Mancini, E., Rizi, V., and Shindell, D. T.: Impact of future climate and emission changes on stratospheric aerosols and ozone, J. Atmos. Sci., 59, 414–440, 2002.

Pyle, D. M., Beattie, P. D., and Bluth, G. J. S.: Sulphur emissions to the stratosphere from explosive volcanic eruptions, Bull Volcanol., 57, 663–671, 1996.

Rahn, T. and Wahlen, M.: Stable isotope enrichment in stratospheric nitrous oxides, Science, 278, 1776–1778, 1997.

Robock, A., Oman, L., and Stenchikov, G. L.: Regional climate responses to geoengineering with tropical and Arctic SO_2 injections, J. Geophys. Res., 113, D16101, doi:10.1029/2008JD010050, 2008.

Rottman, G. J., Woods, T. N., and McClintock, W.: SORCE solar UV irradiance results, Adv. Space Res., 37, 201–208, 2006.

Savarino, J., Romero, A., Cole-Dai, J., Bekki, S., and Thiemens, M. H.: UV induced mass-independent sulfur isotope fractionation in stratospheric volcanic sulfate, Geophys. Res. Lett., 30, 2131, doi:10.1029/2003GL018134, 2003.

Sidhu, K. S., Csizmadia, I. G., Strausz, O. P., and Gunning, H. E.: The reactions of sulfur atoms. VII. The ultraviolet spectrum, the photolysis, and the mercury sensitization of carbonyl sulfide, J. Amer. Chem. Soc., 88, 2412–2417, 1966.

SPARC: SPARC Assessment of Stratospheric Aerosol Properties (ASAP), edited by: Thomason, L. and Peter, T., Tech. Rep. WMO-TD No. 1295, WCRP Series Report No. 124, SPARC Report No. 4, Berrieres le Buisson Cedex, 2006.

Suzuki, T., Katayanagi, H., Nanbu, S., and Aoyagi, M.: Nonadiabatic bending dissociation in 16 valence electron system OCS, J. Chem. Phys., 109, 5778–5794, 1998.

Tanaka, N., Xiao, Y. T., and Lasaga, A. C.: Ab initio study on carbon Kinetic Isotope Effect (KIE) in the reaction of CH_4+Cl, J. Atmos. Chem., 23, 37–49, 1996.

Turco, R. P., Cicerone, R. J., Inn, E. C. Y., and Capone, L. A.: Long wavelength carbonyl sulfide photo-dissociation, J. Geophys. Res., 86, 5373–5377, 1981.

Turco, R. P., Whitten, R. C., Toon, O. B., Pollack, J. B., and Hamill, P.: OCS, stratospheric aerosols and climate, Nature, 283, 283–286, 1980.

Ueno, Y., Johnson, M. S., Danielache, S. O., Eskebjerg, C., Pandey, A., and Yoshida, N.: Geological sulfur isotopes indicate elevated OCS in the Archean atmosphere, solving faint young sun paradox, P. Natl. Acad. Sci. USA, 106, 14784–14789, 2009.

Van Hook, W. A.: Kinetic isotope effect: Introduction and discussion of the theory, editd by: Collins, C. J. and Bowman, N. S., Isotope effect in chemical reactions, Van Nostrand Reinhold, CO, New York, USA, 1970.

Weisenstein, D. K., Yue, G. K., Ko, M. K. W., Sze, N.-D., Rodriguez, J. M., and Scott, C. J.: A two-dimensional model of sulfur species and aerosols, J. Geophys. Res., 102, 13019–13035, 1997.

Wiebe, H. A., Knight, A. R., Strausz, O. P., and Gunning, H. E.: The reactions of sulfur atoms. V. Further studies on the reactions with olefins, J. Amer. Chem. Soc., 87, 1443–1449, 1964.

Zhao, Z., Stickel, R. E., and Wine, P. H.: Quantum yield of carbon monoxide production in the 248 nm photodissociation of carbonyl sulfide (OCS), Geophys. Res. Lett., 22, 615–618, 1995.

Zmolek, P., Xu, X. P., and Jackson, T.: Large mass independent sulfur isotope fractionations during the photopolymerization of (CS_2)-C-12 and (CS_2)-C-13, J. Phys. Chem. A, 103, 2477–2480, 1999.

Table 1. Results for OCS photolysis experiments

Run-ID	OCS	Time	N_2	λ	S^0 Yield	S^0			Residual OCS			f		$^{34}\varepsilon$ (‰)	
	(mbar)	(min)	(mbar)	(nm)	(μmol)	$\delta^{33}S$	$\delta^{34}S$	$\delta^{36}S$	$\delta^{33}S$	$\delta^{34}S$	$\delta^{36}S$	Yield[a]	MB[b]	Yield[a]	MB[b]
07-25	22.5	60			n.d.	−3.25	−6.17	−11.51	0.77	1.44	2.67		0.81		−6.9
09-17	24.5	180			271.4	−1.78	−3.47	−6.95				0.53		−4.8	
10-02	11.5	60			65.2	−3.37	−6.08	−11.43	0.95	1.67	3.15	0.76	0.78	−7.0	−6.9
10-03	6.9	60			66.6	−3.14	−5.77	−11.15	2.48	4.43	8.49	0.59	0.57	−7.6	−7.7
10-23	85.3	60			78.4	−3.14	−5.77	−12.17				0.96		−5.9	
10-29	3.9	60			66.9	−1.38	−2.24	−4.52				0.26		−4.7	
11-05	4.1	30			6.8	−3.03	−5.55	−10.99	1.35	2.5	4.84	0.93	0.69	−5.8	−6.7
11-11	25.3	10			21.3	−3.61	−6.72	−12.7	0.02	0.01	−0.05	0.96	1.00	−6.9	−6.7
10-19	19.5	60	53.3		50.3	−2.51	−4.97	−10.79				0.89		−5.3	
11-10	26.1	60	401		94.8	−2.97	−5.46	−10.93				0.85		−5.9	
11-12	3.7	30	405		18.9	−3.25	−5.99	−11.46	0.21	0.26	0.5	0.78	0.96	−6.8	−6.1
11-28	501	48 hr		>285	68.9	−4.85	−9.49	−19.39	−0.19	−0.37	−0.85	0.99	1.04	−9.5	−9.3

[a] residual OCS derived from S^0 yield. [b] that derived from isotope mass balance.

Table 2. Kinetic isotope effects for sulfur abstraction reactions estimated by the transition state theory.

Reaction	$^{33}\varepsilon_2$	$^{34}\varepsilon_2$	$^{36}\varepsilon_2$	$^{33}\theta$	$^{36}\theta$
$OC^xS + S \rightarrow TS1 \rightarrow CO + {}^xSS$	−9.76	−18.94	−35.86	0.5131	1.910
$OC^xS + S \rightarrow TS2 \rightarrow CO + {}^xSS$	−1.60	−3.10	−5.88	0.5144	1.900

Table 3. Isotope effects for OCS photolysis as a function of OCS pressure estimated from the ZPE-shift method.

Pressure (mbar)	$^{33}\varepsilon_1$	$^{34}\varepsilon_1$	$^{36}\varepsilon_1$	$^{33}\theta$	$^{36}\theta$
2.7	−0.70	−1.35	−2.56	0.5135	1.901
13.3	−0.93	−1.80	−3.41	0.5139	1.899
26.7	−1.12	−2.19	−4.15	0.5139	1.899
400	−2.09	−4.06	−7.69	0.5139	1.898

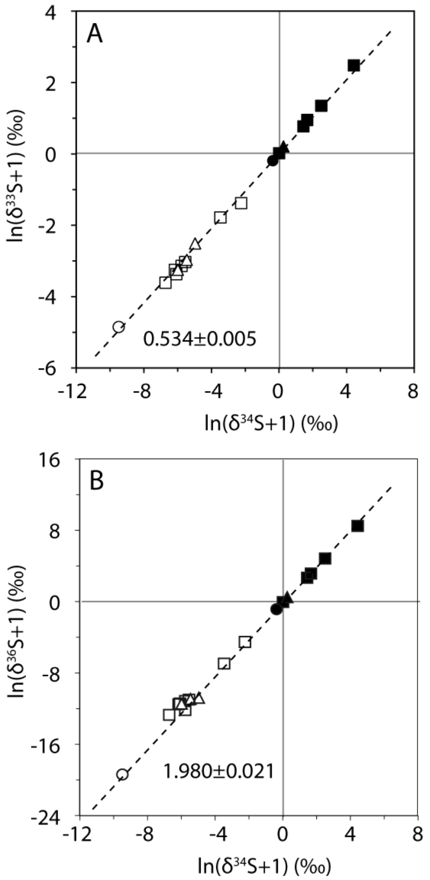

Fig. 1. Sulfur isotopic compositions of residual OCS (filled symbols) and product S^0 (open symbols) relative to initial OCS after photolysis of OCS. Square, triangle, and circle symbols are for pure OCS, OCS with N_2, and OCS with $\lambda>285$ nm photolysis experiments, respectively.

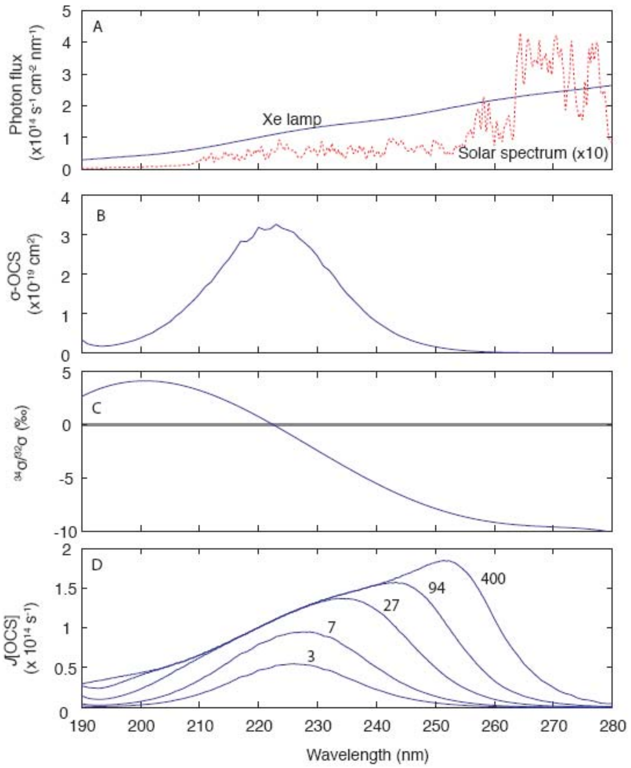

Fig. 2. Input parameters for the models for isotope fractionation. **(A)** Comparison of photon flux of Xe arc lamp (solid line) and solar spectrum (dashed line from Rottman et al., 2006). **(B)** OCS cross section from Molina et al. (1981). **(C)** cross section ratio $^{34}\sigma/^{32}\sigma$ estimated from ZPE-shift method. **(D)** photolysis rate as a function of OCS pressure (numbers in diagram in mbar).